Spin-dependent Hubbard model and a quantum phase transition in cold atoms

W. Vincent Liu,[1] Frank Wilczek,[1] and Peter Zoller[2]
[1]*Center for Theoretical Physics, Department of Physics, Massachusetts Institute of Technology, Cambridge, Massachusetts 02139, USA*
[2]*Institut für Theoretische Physik, Universität Innsbruck, A-6020 Innsbruck, Austria*
(Received 11 May 2004; published 13 September 2004)

We describe an experimental protocol for introducing spin-dependent lattice structure in a cold atomic Fermi gas using lasers. It can be used to realize Hubbard models whose hopping parameters depend on spin and whose interaction strength can be controlled with an external magnetic field. We suggest that exotic superfluidities will arise in this framework. An especially interesting possibility is a class of states that support coexisting superfluid and normal components, even at zero temperature. The quantity of normal component varies with external parameters. We discuss some aspects of the quantum phase transition that arises at the point where it vanishes.

DOI: 10.1103/PhysRevA.70.033603 PACS number(s): 03.75.Ss, 32.80.Pj, 74.20.−z

I. INTRODUCTION

Cold-atom systems can be used to explore important problems of condensed matter physics in new ways. For example, recent rapid development of the ultracold atomic gas in optical lattices [1,2] supported the observation of the superfluid–Mott insulator transition in cold atomic bosons confined in an optical lattice [3–6]. In a wider context, methods of "engineering" various lattice model systems with bosonic and fermionic atoms have been proposed [7–16], opening prospects for exploring exotic new phases. In recent years achieving superfluidity in cold atomic *fermions* has become a major goal, involving several experimental programs [17–25]. Here we consider techniques that permit one to introduce both sorts of complexity in one system, with controlled band structures and interactions that depend on spin. They involve counterpropagating laser beams that together generate a standing light wave which leads to different ac Stark shifts for the spin-up and spin-down components of alkali-metal atoms (such as ^{40}K) in their ground state [2,8]. We then discuss an interesting new phase of matter that might arise in this context, involving coexistence of normal Fermi liquid and superfluid components [26–32], and the quantum phase transition between this state and conventional Bardeen-Cooper-Schrieffer [33] (BCS) superfluidity.

II. SPIN-DEPENDENT OPTICAL LATTICES FOR COLD FERMIONIC ATOMS

In this section we describe how to realize, using cold atoms in an optical lattice, a rather general band Hubbard-type model, with separate, tunable effective masses and filling factors for the two spins [7,8,15].

A. The setup of an optical lattice model

Atoms in an off-resonant laser field exhibit a second-order ac Stark shift of their ground state levels. This shift is proportional to the light intensity. The intensity may vary in space, for example, by forming a standing light wave from counterpropagating laser beams. For the center-of-mass motion of the atoms, spatially varying ac Stark shifts play the role of a conservative potential. In particular, a standing light wave leads to a periodic intensity pattern which results in a periodic potential, i.e., an optical lattice. By superimposing lattice beams from different directions and different intensity an effectively one- (1D), two- (2D), or three-dimensional (3D) lattice can be built.

Consider a cloud of cold fermionic atoms in a 3D optical lattice [15]. We assume that only two of the internal ground states participate in the dynamics, which we call spin up and down, $|\uparrow\rangle$ and $|\downarrow\rangle$. The corresponding effective Hamiltonian is

$$H = \sum_{\sigma} \int d^3x \psi_{\sigma}^{\dagger}(\mathbf{x}) \left[-\frac{\hbar^2}{2m}\nabla^2 + V_{\sigma}(\mathbf{x}) \right] \psi_{\sigma}(\mathbf{x}) - \delta \int d^3x \psi_{\uparrow}^{\dagger}(\mathbf{x})\psi_{\uparrow}(\mathbf{x}) + \frac{\Omega_0}{2} \int d^3x \psi_{\uparrow}^{\dagger}(\mathbf{x})\psi_{\downarrow}(\mathbf{x}) + \text{H.c.} + \frac{4\pi a_s \hbar^2}{m} \int d^3x \psi_{\uparrow}^{\dagger}(\mathbf{x})\psi_{\downarrow}^{\dagger}(\mathbf{x})\psi_{\downarrow}(\mathbf{x})\psi_{\uparrow}(\mathbf{x}), \quad (1)$$

with $\psi_{\sigma=\uparrow,\downarrow}(\mathbf{x})$ fermionic field operators obeying the usual anticommutation relations. The various terms contributing to the Hamiltonian are illustrated in Fig. 1.

The first line in Eq. (1) contains the kinetic energy and the optical lattice potential $V_{\sigma}(\mathbf{x})$ generated by the laser beams, obtained in second-order perturbation theory for coupling of the ground state levels to the excited atomic states. In the simplest case of three orthogonal laser beams this potential has the form

$$V_{\sigma}(\mathbf{x}) = \sum_{\ell=1}^{3} V_{\sigma\ell}^{(0)} \sin^2 kx_{\ell}. \quad (2)$$

Here $k=2\pi/\lambda$ is the wave vector of the light, and $V_{\sigma\ell}^{(0)}$ is proportional to the lattice beam intensity in the direction ℓ and the dynamic atomic polarizability at the laser frequency of the level (spin state) σ.

Note that in Eq. (1) we have ignored *cross* ac Stark terms coupling two different spin components. These are negligible for the situation indicated in Fig. 2, where the ac Stark shifts are much smaller than the (bare) energy of the atomic levels,

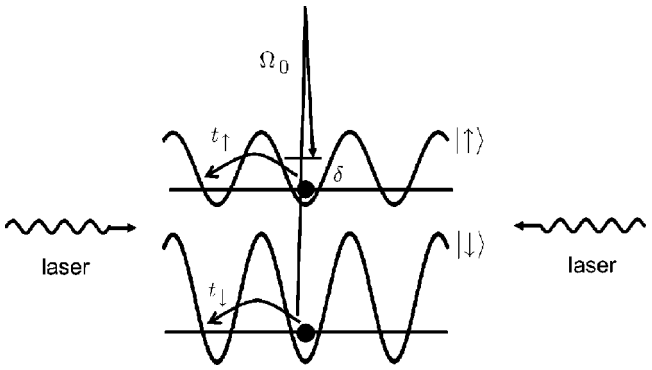

FIG. 1. Spin-dependent lattice: two counterpropagating laser beams generate a standing light wave which leads to different ac Stark shifts for the spin-up and spin-down components of the ground state atoms ($\sigma=\uparrow,\downarrow$). As a result the tunneling matrix elements t_σ for the two spin components are different. The spin-up and -down components are coupled by a Raman laser with Rabi frequency Ω_0 and detuning δ.

which can be achieved, e.g., by applying a magnetic field to split the magnetic sublevels of the atoms. Furthermore, we have assumed in Eq. (2) that the ac Stark shifts of lattice beams in different directions can be added. Depending on the laser configuration there may be interference terms. However, for lattice beams in different directions with (slightly) shifted optical frequencies (obtained by modulating the lattice beams), these interference terms will average to zero. We have also ignored contributions from spontaneous emission. These can, for sufficiently large detunings of the lattice beams from the excited states, be made arbitrarily small. Indeed, for large detuning $\Delta \gg \Gamma$ from excited states with width Γ, the spontaneous emission rate scales as Γ/Δ^2 while the lattice potential scales as $1/\Delta$, so spontaneous emission becomes, on the relevant dynamical time scale, negligible.

A key element in Eq. (1) is the assumption that the lattice potential $V_\sigma(\mathbf{x})$ is spin dependent, as illustrated graphically in Fig. 1. Immediately below we will discuss in detail specific atomic and laser configurations that allow us, by varying laser parameters, to engineer this spin dependence.

The second line in Eq. (1) describes the coupling of the two spin states via a Raman transition with effective two-photon Rabi frequency Ω_0, and Raman detuning δ. The Hamiltonian has been written in the frame where the optical frequencies have been transformed away, so that only the detuning δ appears in Eq. (1).

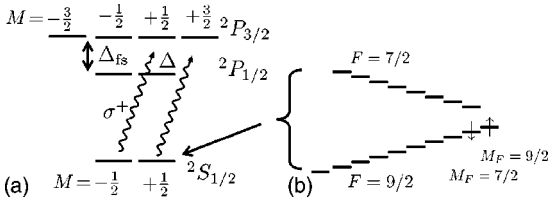

FIG. 2. (a) Atomic level scheme of alkali-metal atoms. A σ^+ polarized lattice beam is tuned between the two excited state fine structure components resulting in different ac Stark shifts for the ground state levels as explained in the context of Eq. (4). (b) Two possible "spin-up" and "spin-down" states are illustrated the case of ^{40}K atoms.

Finally, the last term in Eq. (1) is the usual atom-atom interaction described by a pseudopotential with scattering length a_s. In atomic experiments the sign and magnitude of the scattering length can be manipulated, for example, with an external magnetic field via Feshbach resonances [21–23]. The derivation of Eq. (1) assumes explicitly that the scattering length is much smaller than the lattice spacing (given by $\lambda/2$). In more general circumstances, the interaction will extend beyond nearest neighbors.

For single atoms the energy eigenstates in the optical lattice are conveniently described by a band structure and Bloch wave functions. An appropriate superposition of the Bloch wave functions forms a set of Wannier states which are localized at the various lattices sites. For typical experimental parameters the frequencies associated with dynamics of cold atoms in the lattice are much smaller than the excitation energies in the optical potential (excitation to higher Bloch bands). Expanding the field operators in the set of Wannier functions of the lowest Bloch band, $\psi_\sigma(\mathbf{x}) = \Sigma_i w_\sigma(\mathbf{x}-\mathbf{x}_i)a_{\sigma i}$, we obtain the Hubbard (single-band) Hamiltonian [7]

$$H = -\sum_{\sigma\langle i,j\rangle} t_\sigma (c^\dagger_{\sigma i} c_{\sigma j} + \text{H.c.}) + h\sum_i (c^\dagger_{\uparrow i} c_{\uparrow i} - c^\dagger_{\downarrow i} c_{\downarrow i}) + \frac{\Omega_0}{2}\sum_i (c^\dagger_{\uparrow i} c_{\downarrow i} + \text{H.c.}) - U\sum_i c^\dagger_{\uparrow i} c^\dagger_{\downarrow i} c_{\downarrow i} c_{\uparrow i}. \quad (3)$$

In the Hamiltonian (3), $h=-\delta/2$ plays the role of "magnetic field," t_σ is a spin-dependent hopping term which follows from the spin-dependent optical potential, and U is an on-site interaction. The dependence of the hopping amplitude t_σ and on-site interaction U on the optical lattice parameters is given by $t_\sigma = E_R(2/\sqrt{\pi})(V_{0\sigma}/E_R)^{3/4}\exp[-2(V_{0\sigma}/E_R)^{1/2}]$ and $U = E_R k a_s \sqrt{8/\pi}(V_{0\sigma}/E_R)^{3/4}$ with $E_R = \hbar^2 k^2/2m$ the recoil frequency of the atoms and $k = 2\pi/\lambda$ the wave vector of the light. Thus the ratio of tunneling to on-site interaction can be controlled via the depth of the optical lattice.

B. Tuning spin-dependent tunneling

For alkali-metal atoms, i.e., the atoms used in present cold Fermi gas experiments, the difficulty in obtaining a *spin-dependent* lattice arises from the *s*-wave character of the ground state. It implies that the ac Stark shift induced by far-off-resonant driving fields is the same for all (hyperfine) ground state levels. Fortunately, however, heavy alkali-metal atoms such as ^{40}K, have a large fine structure splitting of the first excited state [34]. This permits us to obtain a spin-dependent optical potential by tuning the lattice lasers between the fine structure levels, still remaining far off resonance to suppress spontaneous emission [8]. As illustrated in Fig. 2, the ground $n\,^2S_{1/2} M = \pm 1/2$ states couple to excited states $n\,^2P_{3/2,1/2}$ with right (left) circularly polarized light σ according to the selection rules $\Delta M = \pm 1$. This gives rise to a spin-dependent ac Stark shift.

For example, the ac Stark shift of the two ground states in circularly polarized light with amplitude $\mathcal{E}$ is

$$\Delta E_{^2S_{1/2}M=+1/2}(\sigma^+) = \frac{|\mu_{3/2}\mathcal{E}|^2}{\hbar(\Delta - \Delta_{\rm fs})}, \quad (4)$$

$$\Delta E^{2}_{S_{1/2}M=-1/2}(\sigma^{+}) = \frac{|\mu_{1/2}\mathcal{E}|^2}{\hbar\Delta} + \frac{|\mu_{3/2}\mathcal{E}|^2}{\hbar(\Delta-\Delta_{\rm fs})},$$

keeping only the dominant contributions from the lowest-lying excited states. Here the detuning from the $^2P_{3/2}$ state is denoted Δ, $\Delta_{\rm fs}$ is the fine structure splitting, and the dipole matrix elements for the transitions from the ground state are $\mu_{3/2,1/2}$. We see that for detunings between the fine structure states $0<\Delta<\Delta_{\rm fs}$ the ac Stark shift $\Delta E^{2}_{S_{1/2}M=-1/2}$ switches from positive to negative values, while $\Delta E^{2}_{S_{1/2}M=+1/2}$ is always negative, giving rise to a strongly spin-dependent lattice potential. We can vary the strength of the Stark shift by varying the laser power.

Thus, the laser configuration consisting of unbalanced right and left circularly polarized polarization components gives rise to a spin-dependent lattice, where the resulting ac Stark shifts are a sum of the shifts in the first and second lines of Eq. (4), weighted according to their fractions of σ^+ and σ^- components. For linearly polarized light the ac Stark shifts of the two states are equal.

It is easy to include hyperfine splitting of the atomic ground states [8]. Consider an atomic ground state electron which is coupled to a nuclear spin I. The resulting total angular momentum is $F=|I\pm 1/2|$, and the hyperfine ground states have the form $|F,M_F\rangle = a|I,M_F+1/2\rangle|^2S_{1/2}M=-1/2\rangle + b|I,M_F-1/2\rangle|^2S_{1/2}M=+1/2\rangle$, where a and b are Clebsch-Gordan coefficients. Assuming that the Zeeman hyperfine states are split by a constant magnetic field [compare the discussion following Eq. (1)], the ac Stark shift of this state will be the weighted sum $\Delta E_{FM_F} = |a|^2\Delta E^{2}_{S_{1/2}M=-1/2} + |b|^2\Delta E^{2}_{S_{1/2}M=+1/2}$ Thus a pair of hyperfine ground state levels will have a spin-dependent lattice provided that the Clebsch-Gordan coefficients in the decomposition are sufficiently different. These spin-dependent lattices were first proposed for quantum computing purposes by Jaksch *et al.* [8] and recently implemented in experiments with cold Rb atoms by Bloch and collaborators [5].

This shows how to create a 1D spin-dependent lattice in counterpropagating laser beams of unbalanced $\sigma^{\pm}$ polarization. The setup is readily generalized to higher dimensions. For example, a 3D lattice is obtained by first applying a magnetic field to provide a Zeeman splitting of the hyperfine ground states (to suppress the cross ac Stark terms), and then applying three standing wave σ^+ polarized beams which are tilted by 45° relative to the magnetic field. Figures 3 and 4 summarize the corresponding results for the $M_F=9/2$ and $7/2$ hyperfine structure ground states [compare the level scheme in Fig. 2(b)]. For these states the squares of the relevant Clebsch-Gordan coefficients (as defined above) are given by $|a|^2=1/9$ and $|b|^2=8/9$. Figure 3 plots the ac Stark shift of the $M_F=9/2$ (solid line) and $M_F=7/2$ states (dashed line) as a function of the laser detuning Δ. The detuning interval covers the region of the $^2P_{1/2}$ and $^2P_{3/2}$ excited fine structure states, which are separated by $\Delta_{\rm fs}$. We see that for a detuning $\Delta\approx 0.248\Delta_{\rm fs}$ the ac Stark shift of the $M_F=7/2$ state has a zero while the shift of the $M_F=7/2$ varies comparatively slowly. For detunings in the range $0.248<\Delta/\Delta_{\rm fs}<1$ the ac Stark shift of both states $M_F=9/2,7/2$ is negative,

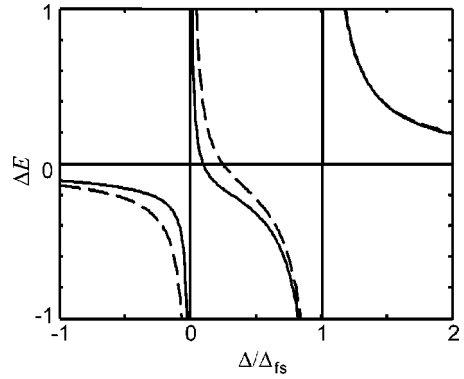

FIG. 3. ac Stark shift (in arbitrary units) of the ^{40}K hyperfine $M_F=9/2$ (solid line) and $M_F=7/2$ (dashed line) states [compare Fig. 2(b)] as a function of the detuning Δ. The value of $\Delta=0$ corresponds to the $^2P_{1/2}$ excited fine structure state, while $\Delta=\Delta_{\rm fs}$ is the $^2P_{3/2}$ resonance. We note the strong spin dependence (i.e., dependence on the internal state) for detuning between the two fine structure states.

i.e., the minima of the optical wells $V_\sigma(\mathbf{x})$ coincide but the wells have different depths, giving rise to a spin-dependent tunneling. The ac Stark shifts in this region between the two fine structure states are plotted in Fig. 4(a) where again the

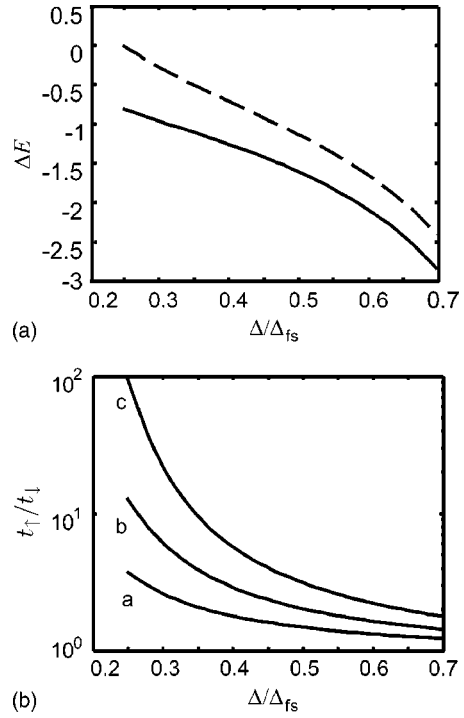

FIG. 4. (a) ac Stark shift (in arbitrary units) of the $M_F=9/2$ (solid line) and the $M_F=7/2$ state (dashed line) in the detuning region right of the interference zero $0.248<\Delta/\Delta_{\rm fs}$ of the $M_F=7/2$ state. (b) Ratio of the hopping matrix elements for the $t_{\uparrow\equiv|M_F=9/2\rangle,\ell}/t_{\downarrow\equiv|M_F=7/2\rangle,\ell}$ for a given spatial direction $\ell=1,2,3$ as a function of detuning Δ for a fixed $V^{(0)}_{\uparrow\equiv|M_F=9/2\rangle,\ell}\equiv V_0$ with $V_0=5$ (curve *a*), 10 (curve *b*), and $20E_R$ (curve *c*) in units of the recoil energy $E_R=\hbar^2k^2/2m$. The hopping matrix elements were obtained from a band structure calculation for the given depth of the optical potential.

$M_F=9/2$ level is represented by the solid line, and the $M_F=7/2$ level of ^{40}K is given by the dashed line. In Fig. 4(b) we give the ratio of the corresponding hopping matrix elements as a function of Δ in the same interval. Here we have chosen a light intensity so that we keep the depth of the optical potential $V^{(0)}_{\uparrow\equiv|M_F=9/2\rangle,\ell}\equiv V_0$ (for a given direction $\ell=1,2,3$) at a fixed given value V_0 for the whole range of detunings, while $V^{(0)}_{\downarrow\equiv|M_F=7/2\rangle,\ell}$ varies. Thus the ratio of $t_{\uparrow\ell}/t_{\downarrow\ell}$ varies. From Fig. 4(b) we see that the ratio of the tunneling elements can be varied by more than an order of magnitude when we approach the interference minimum at $\Delta\approx 0.248\Delta_{\mathrm{fs}}$.

In addition to the alkali-metal atoms discussed above, experimental progress might soon allow the realization of quantum degenerate Fermi gases with alkaline-earth atoms e.g., with Sr atoms [35,36]. Alkaline-earth atoms have, as well as their singlet ground states, long-lived electronic excited triplet states. Applying an off-resonant laser field, these states will in general have quite different ac Stark shifts [37]. Identifying the ground and metastable excited states with the spin-up and spin-down states, we thus can also have a natural realization of a Hubbard model with a spin-dependent interaction.

C. Remarks on spin superposition by Rabi coupling

The model we have been able (conceptually) to engineer contains a Rabi coupling that is not present in the conventional Hubbard model (3). A few remarks about this issue are in order.

$\Omega_0=0$ corresponds to the case that the particle number in each spin species is conserved separately. For $\Omega_0\neq 0$ only total particle number is conserved, while the relative particle numbers can vary. This point will be important for our discussion of exotic phases.

To treat the effect of the Rabi term theoretically, we should first diagonalize the quadratic part of the Hamiltonian. This is best done in momentum space. In principle, we can always find a unitary transformation of the original fermion fields,

$$\tilde{c}_\sigma(\mathbf{k})=\mathcal{U}_{\sigma\sigma'}(\mathbf{k})c_\sigma(\mathbf{k}), \tag{5}$$

that transforms the Hamiltonian into

$$\tilde{H}=\sum_{\mathbf{k}\sigma}\tilde{\epsilon}_{\sigma\mathbf{k}}\tilde{c}^\dagger_{\sigma\mathbf{k}}\tilde{c}_{\sigma\mathbf{k}}-\sum_{\{k_i,\sigma_i\}}V_{\sigma_1,\ldots,\sigma_4;\mathbf{k}_1,\ldots,\mathbf{k}_4}\tilde{c}^\dagger_{\sigma_1\mathbf{k}_1}\tilde{c}^\dagger_{\sigma_2\mathbf{k}_2}\tilde{c}_{\sigma_3\mathbf{k}_3}\tilde{c}_{\sigma_4\mathbf{k}_4} \tag{6}$$

with

$$V_{\sigma_1,\ldots,\sigma_4;\mathbf{k}_1,\ldots,\mathbf{k}_4}=U\delta^d(\mathbf{k}_1+\mathbf{k}_2-\mathbf{k}_3-\mathbf{k}_4)\times\mathcal{U}_{\sigma_1\uparrow}(\mathbf{k}_1)\mathcal{U}_{\sigma_2\downarrow}(\mathbf{k}_2)\mathcal{U}^\dagger_{\sigma_3\uparrow}(\mathbf{k}_3)\mathcal{U}^\dagger_{\sigma_4\uparrow}(\mathbf{k}_4)$$

in d spatial dimensions. The explicit form of the unitary transformation matrix $\mathcal{U}(\mathbf{k})$ for each mode $\mathbf{k}$ can be found easily after some elementary algebra, but is not essential to our discussion here. The important point is that the effective energy bands $\tilde{\epsilon}_{\sigma\mathbf{k}}$ remain spin dependent. The free parameters h, Ω_0, and t_σ allow great freedom of tuning for the band mass ratio and the Fermi surface difference of the effective up and down fermions. Instead of working with the Hamiltonian (3) of the original fermions, we could just as well start with the Hamiltonian (6) of the effective fermions. The interaction term will now contain not only *s*-wave spin-singlet terms, but also other higher angular and spin terms. As far as our main interest, *s*-wave spin-singlet pairing, is concerned, the theoretical treatment does not differ substantially from the model (7) below, for which the Rabi term is transformed away.

III. BREACHED PAIRING TO BCS TRANSITION

Recently there has been considerable discussion of the possible existence of homogeneous zero-temperature phases wherein superfluid condensation coexists with one or more Fermi surfaces, where the gap vanishes. We have in mind that these are full-fledged codimension-1 Fermi surfaces (e.g., two-dimensional surfaces, which bound three-dimensional regions, in a three-dimensional system) where the gap vanishes. The roots of this idea go back to early work of Sarma [38]; the issue has arisen again, under several different names, in several other contexts, including high-density QCD and (as emphasized here) cold-atom systems. There are delicate issues of stability involved, which have been mishandled in much of the literature. We believe that a careful and correct discussion is supplied in Ref. [39]. We shall not repeat the analysis given there, but we rely on the conclusion: there are a number of physically interesting circumstances in which two-component interacting Fermi systems, of the general type discussed in the preceding section, can support a continuous "breached pairing" (BP) to a BCS quantum phase transition (i.e., a "superfluid+normal −superfluid" transition at zero temperature).

Stability of the BP phase, which has coexisting, homogeneous superfluid and normal components at zero temperature, appears to require momentum-dependent interactions, same-species repulsion, or some other complication not present in the simplest Hubbard Hamiltonian with two states defining a quasi spin degree of freedom. For the sake of simplicity and concreteness, however, we shall work with this Hamiltonian. The qualitative, universal features of the phase transition ought not to depend on this idealization. Then,

$$H=-\sum_{\sigma\langle i,j\rangle}t_\sigma(c^\dagger_{\sigma i}c_{\sigma j}+\mathrm{H.c.})+h\sum_i(c^\dagger_{\uparrow i}c_{\uparrow i}-c^\dagger_{\downarrow i}c_{\downarrow i})-U\sum_i c^\dagger_{\uparrow i}c^\dagger_{\downarrow i}c_{\downarrow i}c_{\uparrow i}, \tag{7}$$

where as usual, $c_{\sigma i}$ and $c^\dagger_{\sigma i}$ are fermion annihilation and creation operators at site i, with $\sigma=\uparrow,\downarrow$ indicating two internal quantum states.

The Hamiltonian (7) appears to be a simplified version of (3), by assuming that the Rabi coupling term is transformed away through (5). An important difference is that the spin-up and -down internal states are coherent now. The two quasispin states could well be two hyperfine spin levels for the case of cold atoms, as we discussed in detail above.

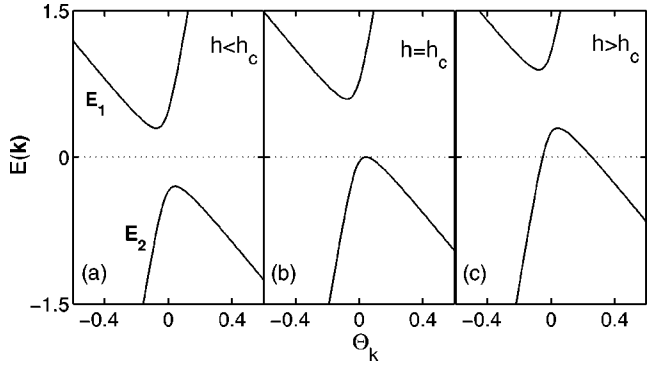

FIG. 5. Quantum phase transition seen from change of quasiparticle spectra. The critical value $h=h_c$ is determined by requiring that the E_2 branch have just one solution at zero energy. For $h>h_c$, one should imagine a three-dimensional momentum space in which two surfaces, defined by $\Theta_{\mathbf{k}}=\Theta^-$ and $\Theta_{\mathbf{k}}=\Theta^+$, are gapless for the E_2 branch. (a) BCS superfluid; (b) quantum critical state; (c) "superfluid+normal" BP state. For convenience, $t_\uparrow \geqslant t_\downarrow$ is always assumed throughout the paper.

A. Nature of quantum phase transition between BCS and BP states

The general nature of the transition can be gleaned from Fig. 5. The BP to BCS transition is continuous, at least in mean field theory. To characterize its critical dynamics, we must use parameters that characterize the singular behavior—in particular, the appearance or disappearance of low-energy degrees of freedom. The magnitude of the superconducting order parameter is evidently not a suitable order parameter, since it evolves smoothly (at the level of mean field theory) and is nonvanishing at both sides of the transition. Furthermore, there is no evident change in symmetry at the transition. We propose that a good order parameter for the BP to BCS transition is the quasispin polarization (see Sec. III D.).

B. Quasiparticle excitations

We shall assume a uniform pairing, with order parameter $\Delta=U\langle c_{i\downarrow}^\dagger c_{i\uparrow}^\dagger\rangle=$const. To find the spectrum of low-energy quasiparticle excitations, we diagonalize the mean field Hamiltonian

$$H_{\mathrm{m}}=\sum_{\mathbf{k}}\Psi_{\mathbf{k}}^\dagger\begin{pmatrix}2t_\uparrow\Theta_{\mathbf{k}}+h-\mu & \Delta\\ \Delta^* & -(2t_\downarrow\Theta_{\mathbf{k}}-h)+\mu\end{pmatrix}\Psi_{\mathbf{k}}, \tag{8}$$

where

$$\Psi_{\mathbf{k}}\equiv\begin{pmatrix}c_{\mathbf{k}\uparrow}\\ c_{-\mathbf{k}\downarrow}^\dagger\end{pmatrix}$$

and

$$\Theta_{\mathbf{k}}=-\sum_{l=1\ldots d}\cos(k_l a).$$

(Here $d=3$ for three-dimensional space.) There are two physical branches of (Bogoliubov) quasiparticle excitations that have distinct properties in a BP state. They are

$$E_{1,2}(\mathbf{k})=(h+t_-\Theta_{\mathbf{k}})\pm\sqrt{(t_+\Theta_{\mathbf{k}}-\mu)^2+|\Delta|^2}, \tag{9}$$

where we have adopted the shorthand notation $t_\pm\equiv t_\uparrow\pm t_\downarrow$. We will assume $t_\uparrow\geqslant t_\downarrow$ and $h>h_\times\equiv-(t_-/t_+)\mu$. By definition, $h_\times$ is the value of the magnetic field for which the spin-up and -down bands have the same Fermi surface.

Figure 5 shows how the two branches of excitations evolve with h. A quantum phase transition takes place at the critical value of $h=h_c$ with [40]

$$h_c=\frac{-\mu t_-+2|\Delta|\sqrt{t_\uparrow t_\downarrow}}{t_+}. \tag{10}$$

An important feature of the BP state is that the E_2 branch of excitations crosses the zero-energy axis at two two-dimensional surfaces in three-dimensional momentum space, defined to be $\Theta_{\mathbf{k}}=\Theta^-$ and $\Theta_{\mathbf{k}}=\Theta^+$. Their values are

$$\Theta^\pm=\frac{(\mu t_+ + h t_-)\pm\sqrt{(h t_+ + \mu t_-)^2-4|\Delta|^2 t_\uparrow t_\downarrow}}{4t_\uparrow t_\downarrow}. \tag{11}$$

At the critical point $h=h_c$, the two gapless "Fermi" surfaces merge into a single one,

$$\Theta^-=\Theta^+=\Theta_c\equiv\frac{\mu t_+ + h_c t_-}{4t_\uparrow t_\downarrow}. \tag{12}$$

Excitation spectra similar to Fig. 5(c) are also found in ferromagnetic metals. It was argued in [41] that superconductivity could coexist with ferromagnetism.

C. As a Lifshitz topological transition

Lifshitz (topological) transitions [42] can take place in metals and alloys at the motion of Van Hove singularities of the electron density of states across Fermi surfaces (for a review, see, e.g., Blanter *et al.* [43]). The transition from a BCS to a BP state actually falls into this universality class.

To illustrate the topological nature of the transition, we start with the many-body wave functions for the BP and BCS states,

$$|\Psi_{\mathrm{BCS}}\rangle=\prod_{\mathbf{k}}(u_{\mathbf{k}}+v_{\mathbf{k}}c_{\mathbf{k}\uparrow}^\dagger c_{-\mathbf{k}\downarrow}^\dagger)|0\rangle, \tag{13}$$

$$|\Psi_{\mathrm{BP}}\rangle=\prod_{\mathbf{k}:\Theta_{\mathbf{k}}<\Theta^-}(u_{\mathbf{k}}+v_{\mathbf{k}}c_{\mathbf{k}\uparrow}^\dagger c_{-\mathbf{k}\downarrow}^\dagger)\prod_{\mathbf{k}:\Theta_{\mathbf{k}}\in[\Theta^-,\Theta^+]}c_{\mathbf{k}\downarrow}^\dagger \times\prod_{\mathbf{k}:\Theta_{\mathbf{k}}>\Theta^+}(u_{\mathbf{k}}+v_{\mathbf{k}}c_{\mathbf{k}\uparrow}^\dagger c_{-\mathbf{k}\downarrow}^\dagger)|0\rangle. \tag{14}$$

Here, $u_{\mathbf{k}}$ and $v_{\mathbf{k}}$ are complex numbers satisfying $|u_{\mathbf{k}}|^2+|v_{\mathbf{k}}|^2=1$; their amplitudes are determined by diagonalizing the mean field Hamiltonian (8),

$$\begin{Bmatrix}|u_{\mathbf{k}}|^2\\ |v_{\mathbf{k}}|^2\end{Bmatrix}=\frac{1}{2}\left(1\pm\frac{t_+\Theta_{\mathbf{k}}-\mu}{\sqrt{[t_+\Theta_{\mathbf{k}}-\mu]^2+|\Delta|^2}}\right). \tag{15}$$

There is a manifold of degenerate states featuring an overall relative phase between the $u_{\mathbf{k}}$ and $v_{\mathbf{k}}$ factors, corresponding

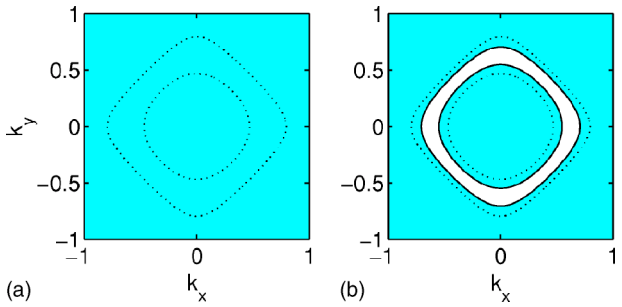

FIG. 6. An illustration of changing topology of the spin-up Fermi sea. Shown are cross sections at $k_z=\pi/2a$ in a 3D first Brillouin zone for (a) BCS and (b) BP; momentum units for k_x, k_y are π/a where a is the cubic lattice constant. As usual, the occupied states spread out over the entire Brillouin zone due to the pairing interaction. The shading in the graph indicates that the region has a nonvanishing occupation number. The dotted lines indicate the orginal free Fermi surfaces of spins up (inner curve) and spins down (outer curve). The solid lines in (b) are energy surfaces defined by $\Theta_{\mathbf{k}}=\Theta^-$ and $\Theta_{\mathbf{k}}=\Theta^+$; for small $\Delta\to 0$, they merge with the free Fermi surfaces (dotted lines). The phase transition occurs at the point in which a simply connected Fermi sea is isolated into two regions.

to the broken $U(1)_{\text{charge}}$. (Note that by our convention of $h>h_\times$, there are more particles in the spin $\downarrow$ species than the $\uparrow$ species.)

The occupation numbers of both spin-up and -down fermions are readily determined. For the BCS state,

$$n_{\mathbf{k}\uparrow}=n_{\mathbf{k}\downarrow}=|v_{\mathbf{k}}|^2 \quad (\text{for all } \mathbf{k}), \tag{16}$$

while for the BP state,

$$n_{\mathbf{k}\uparrow}=0,\ n_{\mathbf{k}\downarrow}=1 \ \text{ if } \ \Theta_{\mathbf{k}}\in[\Theta^-,\Theta^+],$$

$$n_{\mathbf{k}\uparrow}=n_{\mathbf{k}\downarrow}=|v_{\mathbf{k}}|^2 \ \text{ otherwise}. \tag{17}$$

In the BCS state the occupation numbers are equal, while for the BP state they differ. Since the BCS state is maintained for a finite range of parameters, its continuous evolution to the BP state is nonanalytic. This signals a (zero-temperature, quantum) phase transition.

The phase transition is associated with a change in topology of the Fermi sea. This kind of transition is generally known as a Lifshitz transition. As shown in Fig. 6, the quantum phase transition connects states of a simply connected Fermi sea and of two isolated regions.

A transition between superfluid phases of different topology in momentum space is also known to occur in, for instance, the ^{3}He-B phase. There, the superfluid velocity with respect to a container drives a quantum phase transition from a fully gapped state to a state of a (gapless) Fermi surface [44,45].

D. The order parameter

We now come to discuss the order parameter that characterizes the quantum phase transition. It is the spin polarization, $M\equiv\langle S_z(\mathbf{x})\rangle=n_\uparrow-n_\downarrow$. However, unlike the usual Landau-Ginzburg type theory, no obvious spontaneously broken symmetry is involved at the transition. The spin polarization density is given by

$$M=-\int_{\Theta^-}^{\Theta^+} d\Theta N(\Theta), \tag{18}$$

where

$$N(\Theta)\equiv\sum_{\mathbf{k}}\delta(\Theta-\Theta_{\mathbf{k}})$$

plays the role of a (dimensionless) density of states. Near the critical point $h=h_c$, both Θ^- and Θ^+ approach Θ_c. So the spin polarization may be approximated to the lowest order in $h-h_c$ by

$$M\simeq N(\Theta_c)(\Theta^--\Theta^+)=-N(\Theta_c)\frac{\sqrt{(\mu t_-+ht_+)^2-4\Delta^2t_\downarrow t_\uparrow}}{2t_\uparrow t_\downarrow}, \tag{19}$$

$$=-N(\Theta_c)\frac{t_+}{2t_\uparrow t_\downarrow}\sqrt{(h-h_c)(h+h_c-2h_\times)}.$$

The spin polarization may be thought of as being derived from the grand thermodynamical potential Ω by viewing it as a functional of h:

$$M=\frac{\delta\Omega[h]}{\delta h}.$$

This formula can be inverted. Define h_M as the magnetic field for which the above equation has a prescribed value M. Then the quantum effective potential $\Gamma[M]$ is defined (as a functional of M, not h) by the Legendre transformation

$$\Gamma[M]=-hM+\Omega[h],$$

with

$$h=h_M$$

fixed. The form of $\Gamma[M]$ is determined by requiring that the equation of state

$$\frac{\partial\Gamma[M]}{\partial M}=-h_M \tag{20}$$

produce what is equivalent to Eq. (19) upon inverting the latter. This leads to

$$\Gamma[M]=\frac{t_-}{t_+}\mu M+\frac{\Delta\sqrt{t_\uparrow t_\downarrow}}{t_+}\left[|M|\sqrt{1+\left(\frac{M}{M_\Delta}\right)^2}+M_\Delta\text{arcsinh}\left(\frac{|M|}{M_\Delta}\right)\right], \tag{21}$$

where M_Δ is a constant and $M_\Delta\equiv\Delta N(\Theta_c)/\sqrt{t_\uparrow t_\downarrow}$. In deriving Eq. (21), we have treated Δ as a magnetic-field-independent parameter to effectively represent the coupling strength. The effective potential is not analytic in M; the appearance of $|M|$ is a consequence of selecting the physically stable solution of it. The physical origin is due to the presence of two gapless "Fermi" surfaces. For small M (and also $M<0$ in our par-

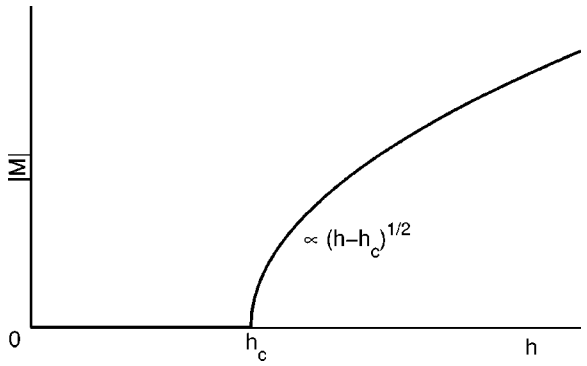

FIG. 7. Quantum phase transition shown by spin polarization M. For the BCS (BP) state, $M=0$ ($M\neq 0$).

ticular case of $t_\uparrow > t_\downarrow$ and $h > h_\times$), we could expand $\Gamma[M]$ in powers of M. Then, in the presence of external magnetic field h, the final effective potential reads

$$V(M) \equiv hM + \Gamma[M] = (h - h_c)M + \frac{\Delta\sqrt{t_\uparrow t_\downarrow}}{3t_+ M_\Delta^2}|M|^3 + \cdots . \tag{22}$$

For $h > h_c$, $V(M)$ always has a minimum at a nonzero M. From either Eq. (19) or Eq. (22), one can immediately verify the following power-law (scaling) relation for the spin polarization at mean field level (for h near h_c)

$$M = \begin{cases} -\dfrac{N(\Theta_c)(t_+\Delta)^{1/2}}{(t_\uparrow t_\downarrow)^{3/4}}(h - h_c)^{1/2} & \text{if } h > h_c, \\ 0 & \text{otherwise}. \end{cases} \tag{23}$$

The results are sketched in Fig. 7. The behavior of spin polarization near the point $h=h_c$ suggests that the quantum phase transition is of second order.

E. Scaling theory of $z=2$ gapless fermions

At the critical point, the $E_2(\mathbf{k})$ branch of quasiparticle excitations is gapless at a single "Fermi surface" defined by $\Theta(\mathbf{k})=\Theta_c$. What makes the critical point special is that the spectrum disperses quadratically near the surface:

$$-E_2(\mathbf{k}) = \frac{\boldsymbol{l}^2}{2m_2^*}, \quad \mathbf{k} \equiv \mathbf{K} + \boldsymbol{l}, \tag{24}$$

where $\mathbf{K}$ is a vector on the critical Fermi surface and $\boldsymbol{l}$ a vector of (small) fluctuating momentum orthogonal to the Fermi surface. m_2^* is the effective band mass which is implicitly determined from Eq. (9). The dispersion relation implies that the dynamical exponent is $z=2$ (at least at the tree-graph level) in contrast with $z=1$ in a nominal (metallic) Fermi liquid [46].

The critical properties of the $E_2(\mathbf{k})$ fermions appear to define a different universality class. To begin understanding it, let us consider the relevant operators. Consider a theory of gapless fermions described by an effective free action plus possible quartic interactions,

$$I_\psi = \int dt d^{d-1}\mathbf{K} d\boldsymbol{l}\psi^\dagger(\mathbf{k})\left(i\partial_t - \frac{\boldsymbol{l}^2}{2m_2^*}\right)\psi(\mathbf{k}) + g\int dt \prod_{j=1\ldots4}[d^{d-1}\mathbf{K}_j d\boldsymbol{l}_j]\psi^\dagger(\mathbf{k}_1)\psi^\dagger(\mathbf{k}_2)\psi(\mathbf{k}_3)\psi(\mathbf{k}_4) \times \delta^d(\mathbf{k}_1 + \mathbf{k}_2 - \mathbf{k}_3 - \mathbf{k}_4) + \psi\psi\psi\psi + \psi^\dagger\psi\psi\psi\cdots, \tag{25}$$

where ψ is the gapless fermion field.

One can perform a simple renormalization group analysis to find out how the interactions should scale. When we scale down the fluctuating momentum $\boldsymbol{l}$ by a factor $s<1$,

$$\boldsymbol{l} \to s\boldsymbol{l},$$

the quasiparticle energy scales down with a dynamical exponent $z=2$ as

$$\omega \to s^2\omega$$

for a quadratic dispersion relationship. So, in geneneral, the momentum and time in the above action should scale as follows:

$$dt \to s^{-2}dt,\ d^{d-1}\mathbf{K} \to s^0 d^{d-1}\mathbf{K},\ d\boldsymbol{l} \to s^1 d\boldsymbol{l},$$

$$\partial_t \to s^2\partial_t,\ \boldsymbol{l} \to s\boldsymbol{l} \text{ with} s \to 0.$$

Note that the momentum $\mathbf{K}$, being attached onto the critical Fermi surface, does not scale. Accordingly, the fermion field scales as

$$\psi \to s^{1/2}\psi.$$

The scaling dimension of potential interaction operators can now be derived by straight-forward power counting. We find that a *generic* four-fermion scattering operator is marginal. That is,

$$g \to \begin{cases} s^0 g & \text{(generic scatterings)}, \\ s^{-1}g & \text{(BCS or forward scatterings)}. \end{cases}$$

This result contrasts dramatically with what is found in the standard renormalization group theory of a conventional Fermi liquid (see, for instance, the review by Shankar [46]). In that context, only special momentum configurations are marginal.

We next turn to the scaling property of the order parameter correlation function. We now attempt to derive the critical theory of quantum fluctuations of the order parameter field M. While the static part of it is already derived in Eq. (22), its dynamical part can be obtained by calculating the spin-spin correlation, which is just the fermion polarization bubble diagram, i.e., $\langle S_z(\mathbf{k}, i\omega)S_z(-\mathbf{k}, -i\omega)\rangle = \Pi(\mathbf{k}, i\omega)$ (in imaginary time formalism), where $S_z(\mathbf{k}, i\omega)$ is defined as the Fourier transform of

$$S_{zi} = \frac{1}{2}(c_{\uparrow i}^\dagger c_{\uparrow i} - c_{\downarrow i}^\dagger c_{\downarrow i})$$

at site i and time t. The quadratic part of the action for M is given by $\Pi(\mathbf{k}, i\omega)$. Near the critical point, we find the quantum effective action of M takes the form,

$$S[M] = \int d^d x d\tau \left[\frac{c_t}{2}(\partial_\tau M)^2 + \frac{c_s}{2}(\nabla M)^2 + \frac{r}{2}M^2 + \frac{g}{3!}|M|^3 + \cdots \right], \quad (26)$$

where

$$r = \frac{2(t_\uparrow t_\downarrow)^{3/4}}{N(\Theta_c)(t_+\Delta)^{1/2}}(h - h_c)^{1/2}, \quad g = \frac{2(t_\uparrow t_\downarrow)^{3/2}}{N^2(\Theta_c)t_+\Delta}, \quad (27)$$

and

$$c_t = \frac{\partial\Pi(\mathbf{k}, i\omega)}{\partial(\omega^2)}, \quad c_s = \frac{\partial\Pi(\mathbf{k}, i\omega)}{\partial(\mathbf{k}^2)}, \quad (28)$$

with $k, \omega \to 0$ (long wavelength limit). In deriving the effective action, we have shifted the position of the minima of $V(M)$ to eliminate the linear term of Eq. (22).

One recognizes that the effective theory of spin polarization field M bears superficial resemblance to Fisher's [47] $i\phi^3$ famous field theory of the Yang-Lee edge singularity in a ferromagnetic Ising model. However, the two theories differ fundamentally in that the cubic interaction term here, $|M|^3$, is both nonanalytic and real (as opposed to analytic and purely imaginary.)

Further investigation of the this new critical theory, including interactions between the low-energy fermion modes and the order parameter, is reserved for future work.

ACKNOWLEDGMENTS

We have benefited from discussions with E. Gubankova, S. Sachdev, T. Senthil, X.-G. Wen, and especially Michael Forbes. This work is supported in part by funds provided by the U.S. Department of Energy (DOE) under Cooperative Research Agreement No. DF-FC02-94ER40818. Work at the University of Innsbruck is supported by the Austrian Science Foundation and EU networks.

[1] For a review, see Nature (London) **416**, 205 (2002).
[2] J. I. Cirac and P. Zoller, Phys. Today **57**(3), 38 (2004).
[3] M. Greiner, O. Mandel, T. Esslinger, T. Hänsch, and I. Bloch, Nature (London) **415**, 39 (2002).
[4] C. Orzel, A. K. Tuchman, M. L. Fenselau, M. Yasuda, and M. A. Kasevich, Science **291**, 2386 (2001).
[5] O. Mandel, M. Greiner, A. Widera, T. Rom, T. Hänsch, and I. Bloch, Nature (London) **425**, 937 (2003).
[6] T. Stöferle, H. Moritz, C. Schori, M. Köhl, and T. Esslinger, Phys. Rev. Lett. **92**, 130403 (2004).
[7] D. Jaksch, C. Bruder, J. Cirac, C. Gardiner, and P. Zoller, Phys. Rev. Lett. **81**, 3108 (1998).
[8] D. Jaksch, H. Briegel, J. Cirac, C. Gardiner, and P. Zoller, Phys. Rev. Lett. **82**, 1975 (1999).
[9] M. Lewenstein, L. Santos, M. A. Baranov, and H. Fehrmann, Phys. Rev. Lett. **92**, 050401 (2004).
[10] B. Damski, J. Zakrzewski, L. Santos, P. Zoller, and M. Lewenstein, Phys. Rev. Lett. **91**, 080403 (2003).
[11] A. B. Kuklov and B. V. Svistunov, Phys. Rev. Lett. **90**, 100401 (2003); L.-M. Duan, E. Demler, and M. D. Lukin, Phys. Rev. Lett. **91**, 090402 (2003).
[12] B. Paredes and J. I. Cirac, Phys. Rev. Lett. **90**, 150402 (2003).
[13] A. F. Ho, M. A. Cazalilla, and T. Giamarchi, Phys. Rev. Lett. **92**, 130405 (2004).
[14] J. K. Pachos and E. Rico, e-print quant-ph/0404048.
[15] W. Hofstetter, J. Cirac, P. Zoller, E. Demler, and M. Lukin, Phys. Rev. Lett. **89**, 220407 (2002).
[16] P. Rabl, A. J. Daley, P. O. Fedichev, J. I. Cirac, and P. Zoller, Phys. Rev. Lett. **91**, 110403 (2003).
[17] K. E. Strecker, G. B. Partridge, and R. G. Hulet, Phys. Rev. Lett. **91**, 080406 (2003).
[18] M. Greiner, C. A. Regal, and D. S. Jin, Nature (London) **426**, 537 (2003).
[19] J. Cubizolles, T. Bourdel, S. J. J. M. F. Kokkelmans, G. V. Shlyapnikov, and C. Salomon, Phys. Rev. Lett. **91**, 240401 (2003).
[20] M. W. Zwierlein, C. A. Stan, C. H. Schunck, S. M. F. Raupach, S. Gupta, Z. Hadzibabic, and W. Ketterle, Phys. Rev. Lett. **91**, 250401 (2003).
[21] C. A. Regal, M. Greiner, and D. S. Jin, Phys. Rev. Lett. **92**, 040403 (2004).
[22] M. Bartenstein, A. Altmeyer, S. Riedl, S. Jochim, C. Chin, J. H. Denschlag, and R. Grimm, Phys. Rev. Lett. **92**, 120401 (2004).
[23] M. W. Zwierlein, C. A. Stan, C. H. Schunck, S. M. F. Raupach, A. J. Kerman, and W. Ketterle, Phys. Rev. Lett. **92**, 120403 (2004).
[24] J. Kinast, S. L. Hemmer, M. E. Gehm, A. Turlapov, and J. E. Thomas, e-print cond-mat/0403540.
[25] F. Ferlaino, E. de Mirandes, G. Roati, G. Modugno, and M. Inguscio, Phys. Rev. Lett. **92**, 140405 (2004).
[26] W. V. Liu and F. Wilczek, Phys. Rev. Lett. **90**, 047002 (2003).
[27] S.-T. Wu and S. Yip, Phys. Rev. A **67**, 053603 (2003).
[28] E. Gubankova, W. V. Liu, and F. Wilczek, Phys. Rev. Lett. **91**, 032001 (2003).
[29] W. V. Liu and F. Wilczek, e-print cond-mat/0304632.
[30] P. F. Bedaque, H. Caldas, and G. Rupak, Phys. Rev. Lett. **91**, 247002 (2003).
[31] J. Liao and P. Zhuang, e-print cond-mat/0307516.
[32] B. Deb, A. Mishra, H. Mishra, and P. K. Panigrahi, e-print cond-mat/0308369.
[33] J. Bardeen, L. N. Cooper, and J. R. Schrieffer, Phys. Rev. **108**, 1175 (1957).
[34] B. DeMarco and D. S. Jin, Science **285**, 1703 (1999).
[35] T. Mukaiyama, H. Katori, T. Ido, Y. Li, and M. Kuwata-Gonokami, Phys. Rev. Lett. **90**, 113002 (2003).
[36] X. Xu, T. H. Loftus, J. W. Dunn, C. H. Greene, J. L. Hall, A. Gallagher, and J. Ye, Phys. Rev. Lett. **90**, 193002 (2003).
[37] H. Katori, M. Takamoto, V. G. Pal'chikov, and V. D. Ovsiannikov, Phys. Rev. Lett. **91**, 173005 (2003).

[38] G. Sarma, J. Phys. Chem. Solids **24**, 1029 (1963).
[39] M. M. Forbes, E. Gubankova, W. V. Liu, and F. Wilczek, e-print hep-ph/0405059.
[40] There is another solution, h_{c2}, which also satisfies the equation $\Theta^- = \Theta^+$. $h_{c2} < h_\times$ (compared with $h_c > h_\times$). For $t_\uparrow \gg t_\downarrow$, h_{c2} is typically negative for a chemical potential close to zero; it corresponds to the heavy fermion band having a smaller Fermi surface than the light. That would realize another special limit of BP—one might call it "exterior gap superfluidity." However, the essential physics is unaltered.
[41] N. I. Karchev, K. B. Blagoev, K. S. Bedell, and P. B. Littlewood, Phys. Rev. Lett. **86**, 846 (2001), and references therein.
[42] I. M. Lifshitz, Sov. Phys. JETP **11**, 1130 (1960).
[43] Y. M. Blanter, M. I. Kaganov, A. V. Pantsulaya, and A. A. Varlamov, Phys. Rep. **245**, 160 (1994).
[44] D. Vollhardt, K. Maki, and N. Schopohl, J. Low Temp. Phys. **39**, 79 (1980).
[45] G. Volovik, *The Universe in a Helium Droplet* (Oxford University Press, New York, 2003), Sec. 26.1.2.
[46] R. Shankar, Rev. Mod. Phys. **66**, 129 (1994).
[47] M. E. Fisher, Phys. Rev. Lett. **40**, 1610 (1978).